



Article

Mechanical Characterization and Finite Element Analysis of Hierarchical Sandwich Structures with PLA 3D-Printed Core and Composite Maize Starch Biodegradable Skins

Maria Zoumaki ¹, Michel T. Mansour ², Konstantinos Tsongas ^{1,3} , Dimitrios Tzetzis ^{3,*} and Gabriel Mansour ¹

¹ Laboratory for Machine Tools and Manufacturing Engineering, Department of Mechanical Engineering, Aristotle University of Thessaloniki, 54124 Thessaloniki, Greece; marizoum@meng.auth.gr (M.Z.); k.tsongas@ihu.edu.gr (K.T.); mansour@auth.gr (G.M.)

² School of Production Engineering and Management, Technical University of Crete, 73100 Chania, Greece; mmansour@isc.tuc.gr

³ Digital Manufacturing and Materials Characterization Laboratory, School of Science and Technology, International Hellenic University, 57001 Thessaloniki, Greece

* Correspondence: d.tzetzis@ihu.edu.gr

Abstract: The objective of this research is the fabrication of biodegradable starch-based sandwich materials. The investigated sandwich structures consist of maize starch-based films as skins and biodegradable 3D-printed polylactic filaments (PLA) as the core. To investigate the tensile properties of the skins, conventional and nanocomposite films were prepared by a solution mixing procedure with maize starch and glycerol as the plasticizer, and they were reinforced with sodium montmorillonite clay, cellulose fibers and fiberglass fabric, with different combinations. Test results indicated a significant improvement in the mechanical and morphological properties of composite films prepared with sodium montmorillonite clay in addition with cellulose fibers and fiberglass fabric, with 20 wt% of glycerol. The morphology of the skins was also examined by scanning electron microscopy (SEM). Three orders of hierarchical honeycombs were designed for the 3D-printed core. To investigate how the skin material and the design of the core affect the mechanical properties of the starch-based sandwich, specimens were tested under a three-point bending regime. The test results have shown that the flexural strength of the biodegradable sandwich structure increased with the use of a second order hierarchy core and starch-based skins improved the strength and stiffness of the neat PLA-based honeycomb core. The bending behavior of the hierarchical honeycombs was also assessed with finite element analysis (FEA) in combination with experimental findings. Flexural properties demonstrated that the use of starch-based films and a PLA honeycomb core is a suitable solution for biodegradable sandwich structures.

Keywords: hierarchical honeycomb structure; starch-based sandwich structure; maize starch; bio-composite films



Citation: Zoumaki, M.; Mansour, M.T.; Tsongas, K.; Tzetzis, D.; Mansour, G. Mechanical Characterization and Finite Element Analysis of Hierarchical Sandwich Structures with PLA 3D-Printed Core and Composite Maize Starch Biodegradable Skins. *J. Compos. Sci.* **2022**, *6*, 118. <https://doi.org/10.3390/jcs6040118>

Academic Editor: Francesco Tornabene

Received: 6 March 2022

Accepted: 11 April 2022

Published: 15 April 2022

Publisher's Note: MDPI stays neutral with regard to jurisdictional claims in published maps and institutional affiliations.



Copyright: © 2022 by the authors. Licensee MDPI, Basel, Switzerland. This article is an open access article distributed under the terms and conditions of the Creative Commons Attribution (CC BY) license (<https://creativecommons.org/licenses/by/4.0/>).

1. Introduction

Sandwich-structured composites have important physical, mechanical and thermal properties and are widely used in various high-technology applications [1–3]. A typical sandwich panel is a composite building material, which usually consists of a basic structure of two thin surfaces separated by a low-density core material [4]. The core is the basic building material of the sandwich that is placed between two thin, rigid structured surfaces, commonly called the skin of the sandwich composite. The core material typically has a low density and strength, but its higher thickness provides the sandwich panel with high structural bending stiffness. The purpose of the core material is to support the sandwich so that it does not deform while the two thin skin surfaces stay fixed relative to each other. This results in a solid, homogeneous structure having much more stiffness than the neat core material [4].

Most of the sandwich structures are made of plastic and other non-ecofriendly materials with high energy production processes. In recent decades, the search for recyclable and biodegradable sandwich structures has continued at an increasing rate due to climate change. Several recent studies have been published on the replacement of synthetic polymer resins by natural fibers to reinforce building materials [5–8]. However, there is very little research and literature on the use of natural materials in the construction of sandwich structures. There is also a growing interest in the application of natural fibers and recycled raw materials in the building and construction industry, where natural polymers have been widely used as binding agents to improve mechanical, thermal and other physical properties of different conventional materials, such as cement, concrete, asphalt, etc. [9–11].

Biodegradable natural polymers, due to their physical and chemical properties, are used in many industrial applications; therefore, biopolymers are a possible solution to reduce the environmental pollution caused by the conventional synthetic polymers derived from non-renewable sources, such as petroleum [7,8,12,13]. Polylactic acid (PLA) is a biodegradable thermoplastic (aliphatic) polyester derived from renewable resources, such as maize starch, tapioca roots, potato starch and sugar cane. PLA has a wide range of applications due to its important physical and chemical properties and is extensively used as a base material for the construction of composite sandwich structures [14–17].

Conventional manufacturing processes for (multi-layer) corrugated sandwich structures include compression molding, hot-press molding and vacuum molding [18]. These conventional methods are relatively expensive and difficult to apply on a large scale, because the molds must be made for different design requirements. In addition, it is very difficult to implement complex core designs of sandwich composites using conventional techniques. Additive manufacturing has been of increasing interest to the building and construction industry for the last few years. Additive manufacturing or three-dimensional (3D) printing, as it is more commonly known, is a process of making three-dimensional physical objects from a digital design. In particular, the principle of Fused Filament Fabrication (FFF) is an extrusion of the molten filament (such as molten polymer) and gradual deposition of layers (through syringes or cartridges) and the consequent solidification. Biomaterials can also be used in 3D printing since natural ecofriendly polymer fluids can be used to create solid objects from CAD drawings by building them in layers [19]. The technique of 3D printing is widely used for the construction of complex geometries at a relatively low cost. Researchers have evaluated the advantages and limitations of different methods of construction of sandwich-structured composites and there has been a significant development of additive manufacturing technologies in recent years, which continue to grow due to the flexibility, speed and relatively low cost of innovative architectural and construction applications [20].

A considerable amount of research has been carried out concerning the preparation of fully biodegradable sandwich structures [9,10]. Thus far, the literature has been focused on the preparation and the mechanical properties of fully biodegradable maize starch-based films, but, to the best of our knowledge, studies have not shown if the use of this type of membrane is suitable for ecofriendly sandwich structures. This study focuses on the fabrication of biodegradable starch-based sandwich materials. The structure of the sandwich consists of skins made from maize starch-based films, reinforced with sodium montmorillonite clay particles, cellulose fibers and fiberglass fabric as well as a biodegradable 3D-printed polylactic filament (PLA) core. Regarding the FEA simulation of the sandwich structures, a lot of researchers have approached various engineering and composite structures under different loading conditions [21–24]. Gohari et al. [21] presented an approach toward the localized failure inspection of pressurized ellipsoidal domes made with a woven composite. Another work [23] has utilized inclined piezoelectric actuators to drive the twisting deformation of smart laminated cantilever composite plates/beams, proposed a novel explicit analytical solution for obtaining twisting deformation and optimal shape control and developed a series of simple, accurate and robust finite element (FE) analysis models and realistic electromechanical-coupled FE procedures for verifica-

tion. Gohari et al. [24] developed an analytical solution for the electromechanical flexural response of smart laminated piezoelectric composite rectangular plates encompassing flexible-spring boundary conditions at two opposite edges that can potentially be applied to real-life structural systems, such as smart floors and bridges, and can be used to analyze the flexural deformation response.

The aim of this study is to investigate the development and manufacturing of ecofriendly biodegradable (maize starch-based) sandwich structures. A sandwich-type composite structure usually consists of three materials: the core material, two layers of external skin surface material and the adhesive layer (which connects the skin surfaces to the core structure of the sandwich panel). The geometrical characteristics and chemical composition of the core material essentially determine the overall mechanical behavior of a sandwich structure. The core is usually low strength, but due to its large thickness, it is rigid with high tensile and compressive strength. The two thin outer face sheets of the panel carry most of the bending loads received by the laminate. Often, the most complex sandwich structures consist of the core material and the outer surfaces with many successive layers of materials with different physical, chemical and mechanical properties [4]. In the present work, the physical and mechanical behavior, synthesis and characterization of these biodegradable sandwich panels as well as their composition and structure were investigated. This research work has two main objectives: (a) the development of a sandwich structure using two starch-based nanocomposite films (reinforced with cellulose fibers and fiberglass fabric) as skins and PLA as the core material and (b) an experimental investigation of the physical and mechanical properties, supported by FEA of these sandwich composite panels.

2. Materials and Methods

2.1. Materials

For the experiments, a commercial maize starch (containing approximately 23% amylose) with moisture content 12 wt% [25] was supplied by Nestlé Hellas, Athens, Greece, and it was mixed with commercial glycerol supplied by Mallinckrodt Chemical Works, St. Louis, MI, USA. The sodium montmorillonite clay with a CEC (cation exchange capacity) of 92.6 meq/100 g clay was supplied by Southern Clay Products, Inc., Austin, Texas USA. Cellulose fibers (Sigma Aldrich, St. Louis, MI, USA) were used to prepare the starch-based skins. The conventional composite starch-based films were reinforced with different types of fiberglass fabrics, supplied by Fibremax Ltd., Volos, Greece. For 3D-printed honeycomb preparation, commercial PLA was supplied by BlackMagic3D Inc., New York, NY, USA, while the bio-epoxy adhesive Easy Composites Ltd. LB2-A, Stoke-on-Trent, (UK) was used to produce sandwich structure composites.

2.2. Methods

2.2.1. Preparation of Starch-Based Skins

Nanocomposite starch-based films were prepared by a solution mixing procedure [26]. The starch was plasticized with glycerol and water and the sodium montmorillonite clay (NaMMT) was used as reinforcement on the mechanical properties of the films. The experimental results indicated that both glycerol and clay contents significantly influenced the physical and mechanical properties of starch-based nanocomposite films and their tensile properties were enhanced even at lower clay content [27–30]. The moisture content of starch was constant, and equal to 12 wt% (determined by drying to constant mass). The maize starch (6.5 wt% in dry basis) was dispersed in distilled water (at temperature of 80 °C) containing different levels of glycerol ranging from 10 to 30 wt%. Then, sodium montmorillonite clay was added to the gelatinized starch solution in various amounts so the NaMMT content of the final nanocomposite film was 3, 5 or 10 wt% of the amount of dry starch. The cellulose fibers were dispersed in 75 mL of water in concentrations of 5–20% wt% (based on the amount of dry starch) [31]. Then, the cellulose suspension was mixed with the starch–montmorillonite solution for 10 min at temperature of 75 °C and the fresh films were obtained by casting the hot mixture into custom-made PTFE

plates with dimensions 220×300 mm [27–29]. By dipping fiberglass fabrics in the starch–gelatin matrix, a clear improvement in the physical and mechanical properties of the nanocomposite films was also achieved. For this purpose, grids with a different cell topology were used, i.e., with irregular structure (random orientation glass fibers 0.1 mm thick) and ordered structure (dense braided fiberglass 0.06 mm thick). The final step in the preparation of films involved placing the specimens in an air circulation drying oven at 45°C for about 2 days. For comparison, all samples were stored under controlled conditions of temperature ($\approx 22^\circ\text{C}$) and relative humidity ($\approx 50\%$) for 30 days prior to testing to secure moisture equilibration [26].

2.2.2. Design and Fabrication of FFF-Printed Honeycomb Structures

Hierarchical honeycomb structures were designed in Solidworks™ CAD software (Dassault Systemes, SolidWorks Corporation, Waltham, MA, USA) and exported as STL file. The manufacturing of FFF-printed honeycomb structures was accomplished by using a commercial open source BCN3D Sigma R17 (BCN3D, Barcelona, Spain) 3D printer with a 2.85 mm extrusion nozzle and Ultimaker Cura (Ultimaker, Utrecht, The Netherlands) was used as slicing software. The basic 3D printing parameters for the cellular core of the sandwich structures were the nozzle extrusion temperature and build-plate temperature of 220 and 60°C , respectively. The deposition line (layer) had a height of 0.2 mm, and the deposition line width was 0.4 mm. The optimal printing speed for the manufacturing of the honeycomb cores was selected to be 40 mm/s. Deposition speed was therefore not considered a variable in this study and a constant extrusion velocity was selected for all specimens, based on device parameters (e.g., effective printing range). Additionally, all specimens were fabricated in room temperature conditions.

All honeycomb structures shown in Figure 1 had a constant relative density $\rho = 0.12$. The hexagon's edge length of the regular honeycomb was $a_h = 20$ mm, and the thickness of the cell wall was measured as $t = 2$ mm. The structural arrangement of the hierarchical honeycomb structures can be defined as the ratio of the length of the second order hexagon divided by the length of the initial hexagon, i.e., $\gamma_1 = b_h/a_h \propto \gamma_2 = c_h/a_h$ [32,33]. The 1st order of honeycomb structures had $\gamma_1 = 0.3$ and $t = 1.25$ mm, and in the same way, the honeycomb structure with 2nd order hierarchy had $\gamma_1 = 0.3$, $\gamma_2 = 0.12$ and $t = 0.86$ mm, as demonstrated in Figure 1a. In addition, the cell wall thickness was reduced with the increase in the level of hierarchy in order to maintain the overall relative density constant. These geometrical attributes were kept similar for the FEA simulations undertaken in the following sections. The CAD model of the hierarchical honeycomb cores for the three levels is shown in Figure 1b [34–36].

The final FFF-printed core of the sandwich structures has a length $l = 190$ mm, width $w = 90$ mm and height $h = 6$ mm. The FFF printing process of the core of the hierarchy level is displayed in Figure 2a. The composite skins glued to the FFF-printed hierarchical cores are portrayed in Figure 2a. In Figure 2b, the skins have been examined with a digital optical microscope Dino-Lite AD7013MZT (AnMo Electronics, Hsinchu, Taiwan) and software DinoLite 2.0. Finally, two different regions have been magnified in Figure 2b in order to examine the fiberglass dispersion. This research has been focused on studying the mechanical properties of honeycomb sandwich structures considering the different architecture of each hierarchy, along with the contribution of the external composite material skins.

2.2.3. Tensile Testing

The tensile properties of the starch–cellulose blends were investigated by testing film specimens of each different content of cellulose and fiberglass fabric. The tensile properties of the samples were measured at room temperature (23°C) by utilizing a M500-50AT (Testometric, Rochdale, UK) universal testing machine that was equipped with a 50 kN load of cell. The specimens were tested at a constant rate of 5 mm/min until the specimen was ruptured. At least three specimens were tested for each sample. The tensile properties

of films were determined according to the standard test methods ASTM D882–12 for thin plastic sheeting [37].

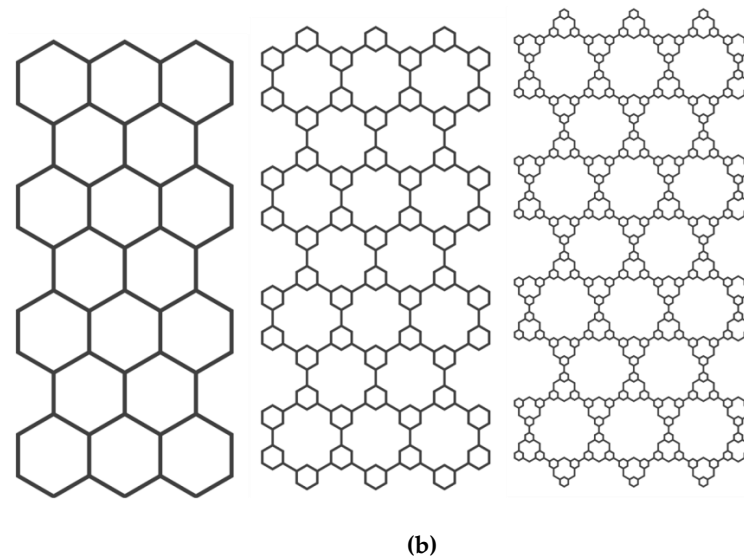
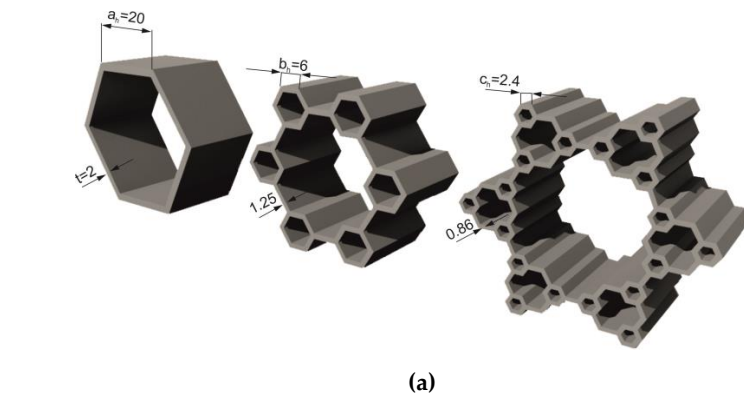


Figure 1. Design of (a) unit cell and (b) hierarchical honeycomb cores.

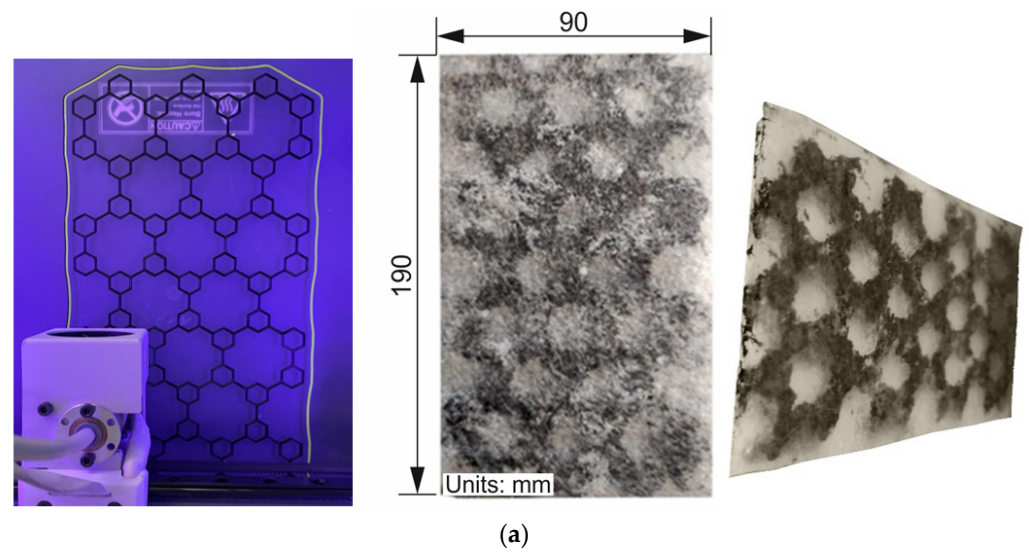


Figure 2. Cont.

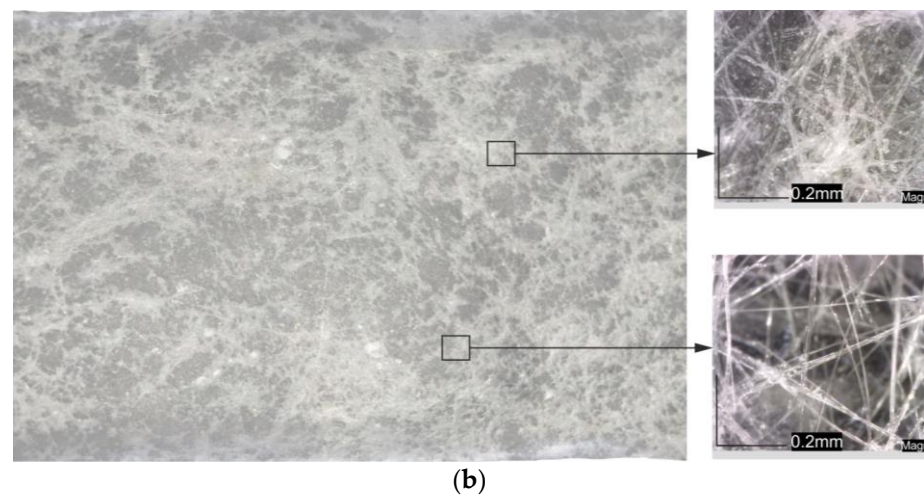


Figure 2. (a) A 3D-printed core (during printing process) and assembly of sandwich structures, (b) top view and optical microscopy of starch-based film (with 20 wt% glycerol, 3 wt% NaMMT, 10 wt% cellulose and fiberglass fabric).

2.2.4. Bending Experiments Assisted by FEA

The bending performance of the 3D-printed sandwich structures with three different hierarchical cores was investigated according to ASTM C393 [38] and it was examined by a universal testing machine Testometric-M500-50AT (Testometric, Rochdale, UK) equipped with a 50 kN load cell. The dimensions of the produced parts for the three-point bending tests are documented in Table 1. The crosshead speed of the experiments was equal to 5 mm/min and the diameter of the supports and the loading pin was 10 mm, as shown in Figure 3a. It is worth mentioning that all experiments were performed three times in order to secure the reliability and the repeatability of the experimental bending results.

Table 1. Dimensions of the produced parts for the three-point bending tests.

Length (mm)	Span Length (mm)	Width (mm)	Core Thickness (mm)	Height (mm)
190	100	90	6	6.8–7

In order to advance the calculation accuracy of the bending tests, a finite element analysis (FEA) model was developed [39–43]. A structural FE analysis based on the ANSYS code was utilized to investigate the deformation process of 3D-printed bending honeycomb structures and extract a constitutive model of their mechanical behavior. Different material parameters were assumed in order to fit the experimental mechanical response of the honeycomb sandwich structures under bending, in terms of force–displacement. The mechanical behavior of the starch-based skins were modeled linearly with an upper strength limit that was defined by the tensile tests, while the PLA honeycomb core was defined by a multilinear stress–strain model. An imposed displacement was applied for each structure. This value corresponds to an experimental displacement from the bending tests. This procedure is repetitive until the last pair of force–depth values are converged, and the solution process ends. The connections of the steel support, the loading pin and the sandwich specimens’ surface were assumed to be frictionless. The surfaces under the supports were considered fixed. The FE model along with corresponding discretization is shown in Figure 3b,c, respectively. The FFF printing defects were neglected during the simulation.

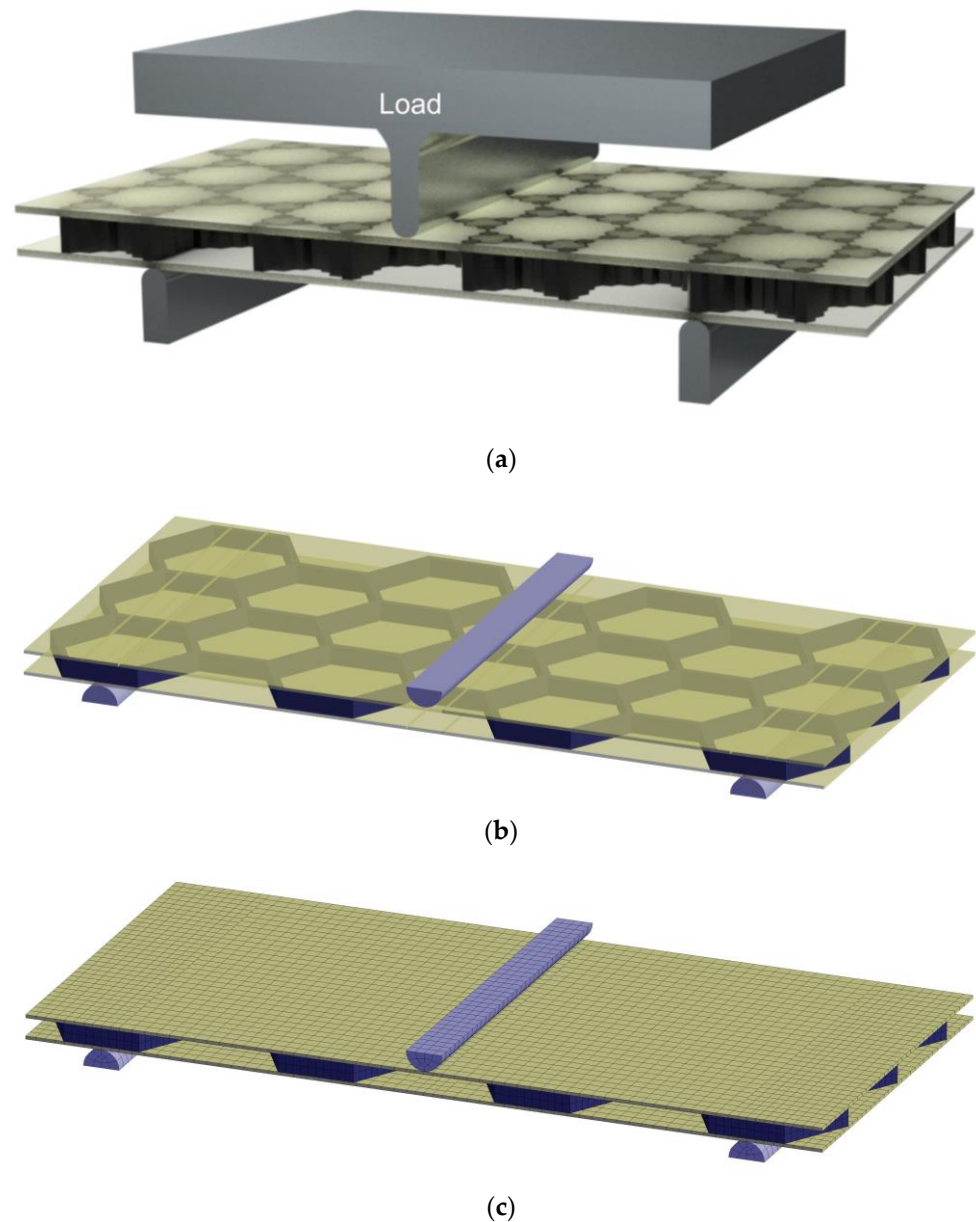


Figure 3. (a) A 3-point bending test set-up illustrated photorealistically with 2nd order hierarchy 3D-printed core assembled between the starch and fiberglass top and bottom skins, (b) CAD geometry of PLA honeycomb structure illustrated with zero level of hierarchy (regular honeycomb), (c) the corresponding mesh used in finite element analysis.

2.2.5. Scanning Electron Microscopy (SEM)

The morphology of the samples was assessed through a Phenom ProX (Thermo-Fisher Scientific, Waltham, MA, USA) instrument, equipped with an optical microscope with a magnification range of 20–135x and a scanning electron microscope (SEM) with a thermionic CeB6 source. A double-sided carbon tape (Ted Pella, Redding, CA, USA) was used to attach the specimens on a metal stub. Then, the metal stub was inserted in the scanning electron microscope's vacuum chamber using a special charge reduction sample holder. The sample holder is designed to reduce sample charging and eliminate extra sample preparation of non-conductive samples. A dedicated software package, ProSuite PC (Thermo-Fisher Scientific, Waltham, MA, USA), was used for the instrument control.

3. Results and Discussion

3.1. Mechanical Properties of Starch-Based Films in Structural Composite Sandwich Panels

The mechanical properties of the films were evaluated initially by experimental mechanical tests. For each sample, three individual replicate starch-based films were obtained, and from each film, four replicate samples were measured. Thus, for each sample, in total, 12 replicates were measured. The measurements were performed at laboratory temperature ($\approx 21\text{--}23\text{ }^\circ\text{C}$). Figure 4 displays stress–strain curves of thermoplastic starch films, where the effects of cellulose, glycerol and NaMMT contents and fiberglass fabric on the mechanical properties of membranes are clearly illustrated.

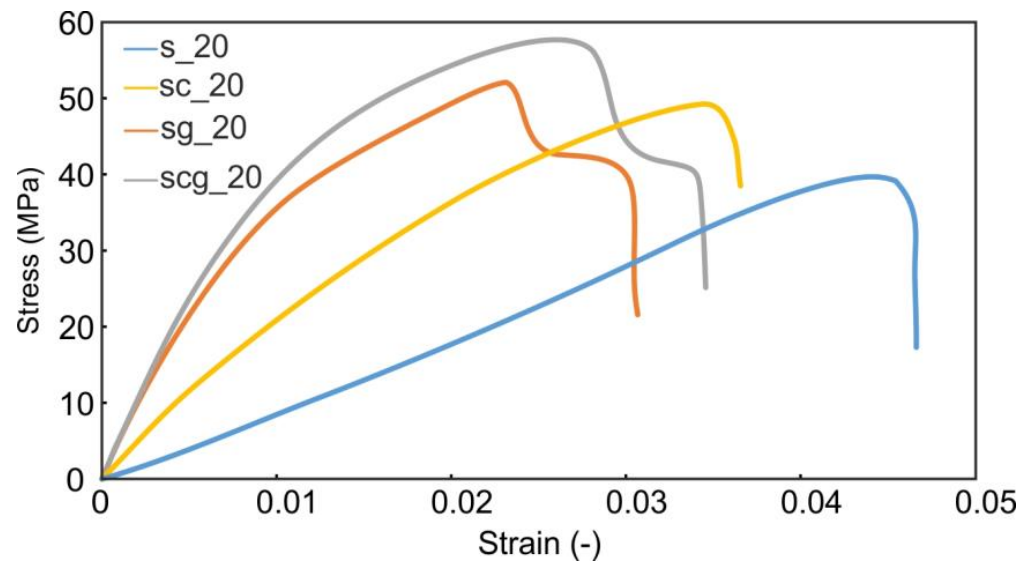


Figure 4. Stress–strain curves of starch films with 20 wt% glycerol, 3 wt% NaMMT and different contents of cellulose and fiberglass fabric.

It is evident from the graph that increasing cellulose content resulted in an increase in tensile strength and elongation at the break of the films. A series of sample starch films with glycerol concentration of 20 $w/w\%$ and NaMMT content of 3% $w/w\%$ are illustrated in Figure 4 for all combinations, i.e., control films (s_20), starch films with 10% w/w cellulose (sc_20) and with fiberglass fabric without cellulose (sg_20).

The experimental results showed that despite the addition of fabric, using a plasticizer in a concentration level of up to 10 wt%, the samples yielded films inhomogeneous, rigid and with cracks, making the film surfaces unable to adhere to the core material. Because the prepared films with 30 wt% glycerol content were macroscopically isotropic, homogeneous, smooth and flexible, it was easier to adhere the films to the surface of a PLA core. However, an increase in glycerol content from 10 to 30 wt% resulted in a significant reduction in the mechanical strength of the sandwich structure. As mentioned in the previous section, the best mechanical results were obtained with a sodium montmorillonite (NaMMT) content of about 10 wt% at a glycerol concentration 20 wt% (scg_20) [26–30,44]. It was also observed that an increase in the size of the membranes (with a clay content of more than 10 wt%) resulted in a stiff/brittle behavior.

As mentioned above, the membranes with maize starch 6.5 wt% in a dry basis, glycerol concentration of 20 wt%, clay content of 3 wt% and fiberglass fabric (with irregular structure) achieved the best physical and mechanical properties and were also used as the skin of the sandwich structure. The experimental results showed that the optimal cellulose content that enhanced the mechanical properties of the films was about 10% wt%. The results of the laboratory tests showed that the combined addition of glycerol and cellulose to the polymer matrix of the starch resulted in the enhancement of mechanical properties of films from 41.9 MPa (s_20) to 45.1 MPa (sc_20). This improvement in film properties was probably

due to the interfacial interaction between the polymeric matrix and clay nanoparticles, due to the chemical similarity of the structure and good compatibility of starch and cellulose that allow for the formation of hydrogen bonding between these polysaccharides [31].

Similar results were obtained in previous studies, where nanocomposite materials were prepared using normal maize starch, plasticized with glycerol and water and reinforced with sodium montmorillonite clay particles and cellulose compounds (carboxymethyl cellulose, CMC) [31]. As it is shown in Figure 4 and Table 2, the use of fiberglass fabric in the film-forming mixture has increased the tensile strength of films from 41.9 MPa (s_20), on average, to 50.52 (sg_20) MPa. However, the samples containing glycerol content of 20 *w/w*% and a layer of fiberglass fabric yielded rigid films with surface cracks. Although incorporating fiberglass fabric had positive effects on the tensile strength, film surfaces became considerably harder and more brittle [41]. The tests showed that with the addition of cellulose, the films can be made softer and more flexible with increasing tensile strength from 45.1 MPa (sc_20) to 55.33 MPa (scg_20), without significantly reducing the elongation at the break (from about 3.7 to 3.3%).

Table 2. Mean values of tensile strength of films prepared.

Sample	Tensile Strength (MPa)
S_20	41.9 ± 1.2
SG_20	50.52 ± 2.1
SC_20	45.1 ± 1.6
SCG_20	55.33 ± 1.9

The experimental results revealed that the starch-based nanocomposite films exhibited enhanced mechanical properties at a glycerol concentration of 20 wt% and clay content of 3 wt%. After a series of laboratory tests to characterize the structure of the sandwich panel, it was concluded that starch-based films with a plasticizer concentration of 20 wt%, sodium montmorillonite content of 3 wt%, cellulose concentration of 10 wt% and fiberglass fabric (with irregular structure) were selected as suitable for bonding films to the PLA surface. This procedure resulted in compact and rigid membranes (0.4–0.5 mm thick) with smooth surfaces and no cracks. The films (in dimensions 90 × 190 mm) were bonded with the adhesive to the surface of a 3D-printed PLA core.

3.2. SEM Analysis of the Starch-Based Skins

The morphology of the obtained samples and the degree of dispersion of cellulose fibers and fiberglass fabric in the plasticized starch matrix were examined by scanning electron microscopy (SEM). SEM micrographs of thermoplastic starch with 20% glycerol, 3% NaMMT and 10% cellulose content (sc_20) are shown in Figure 5. Figure 5a shows thermoplastic starch containing 20% glycerol, 3% NaMMT, 10% cellulose fibers and a layer of fiberglass fabric. The image of thermoplastic starch with 10% cellulose, without the fiberglass layer, shows a compact morphology of swollen granules surrounded by material which presumably consisted of amylose chains, glycerol and water. Figure 5b shows samples including a layer of fiberglass, with a smooth and homogeneous surface. It can be seen that the starch-based films with 10% cellulose with no fiberglass fabric and films with 10% cellulose and fiberglass fabric showed surfaces without noticeable breaks or cracks, with a fairly homogeneous distribution of cellulose fibers and NaMMT particles in the thermoplastic starch matrix with randomly oriented fiberglass fibers.

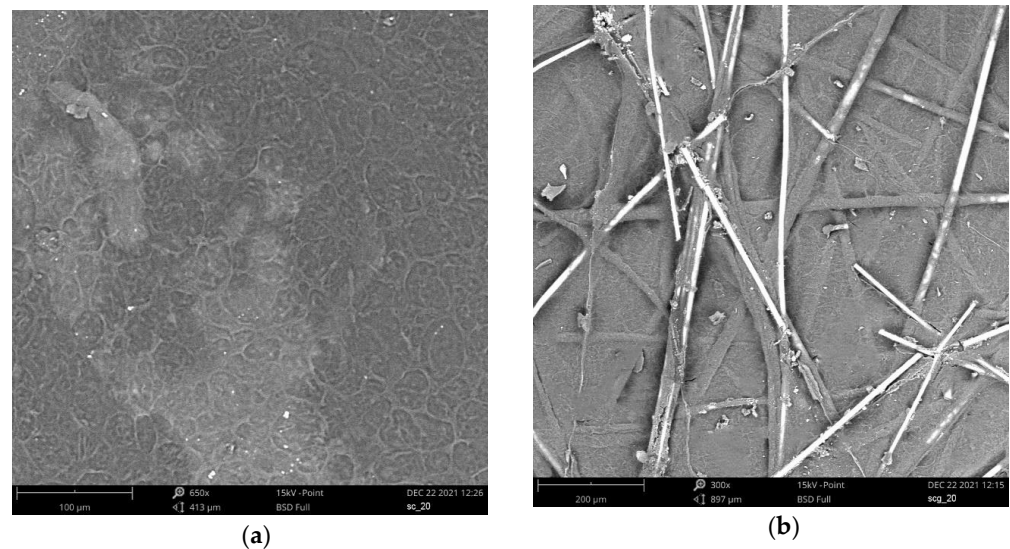


Figure 5. Scanning electron micrographs of starch films containing (a) 20 % glycerol, 3% NaMMT and 10% cellulose and (b) 20% glycerol, 3% NaMMT, 10% cellulose and fiberglass fabric.

3.3. Bending Behavior and FE Analyses

Three different hierarchical honeycomb core structures of the sandwich panels have been FFF printed by biodegradable PLA material in order to study their bending behavior. HC0 represents the zero level of hierarchy (regular honeycomb), HC1 represents the first level of hierarchy and HC2 represents the second level of hierarchy. The compressive behavior of these hierarchical structures along with the FE simulation has been discussed extensively in previous work [33–35]. Static bending loads have been applied to these biodegradable sandwich structures using a Testometric M500-50AT equipped with a 50kN load cell, as shown in Figure 6a,b.

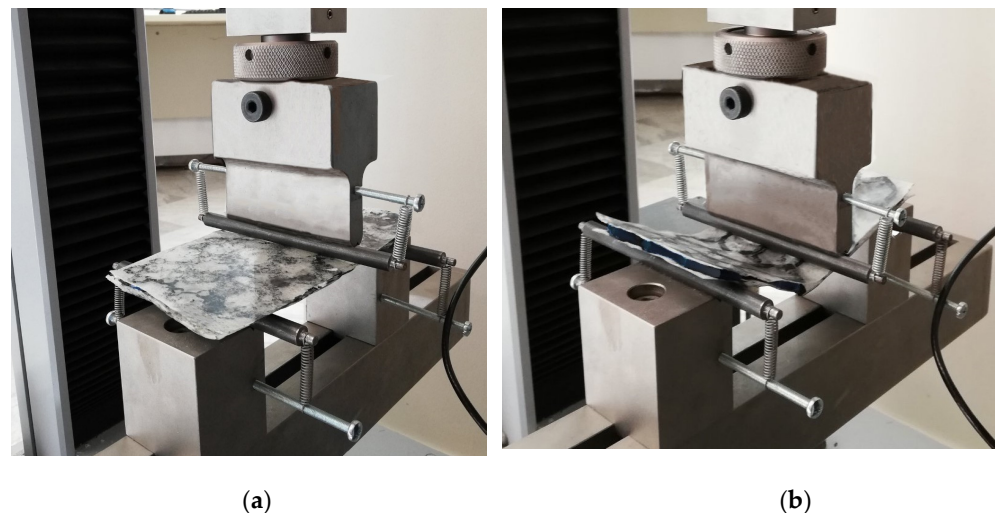
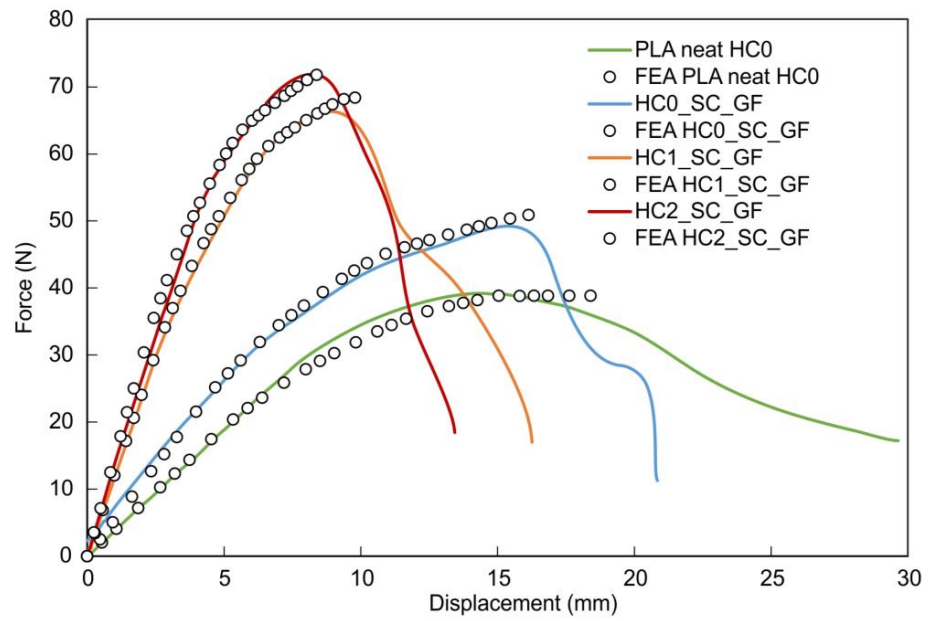
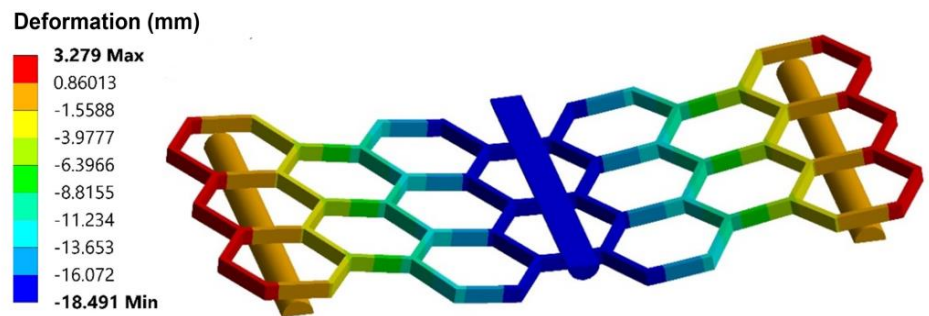


Figure 6. A 3-point bending test on starch-based sandwich structures (a) at zero deformation with no bending load applied and (b) maximum deformation under ultimate bending load.

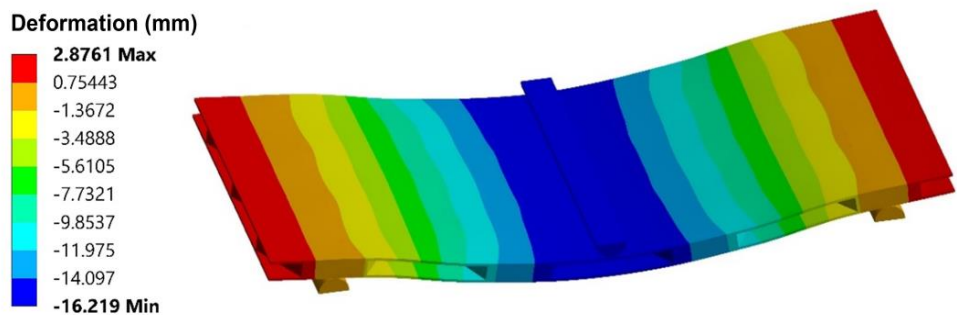
In Figure 7a, the ultimate bending loads were measured to be 39.2 N for PLA, while for the hierarchical sandwich structures PLA/HC0 scg_20, PLA/HC1 scg_20 and PLA/HC2 scg_20, the measured values were 49.9, 65.7 and 72.8 N, respectively. The bending stiffness for the PLA structure has been calculated to be 3.85N/mm, while for the hierarchical sandwich structures PLA/HC0 scg_20, PLA/HC1 scg_20 and PLA/HC2 scg_20, the measured values were 5.42, 12.10 and 14.69 N/mm, respectively.



(a)



(b)



(c)

Figure 7. (a) Force–displacement graphs from 3-point bending tests and curve-fitted data obtained from the FEA, (b) the deformation behavior of the PLA specimens and (c) the deformation behavior of PLA HC0 sandwich specimens.

These results demonstrate an increase in the bending stiffness between regular honeycomb and the other levels of hierarchy. Specifically, the bending stiffness of PLA/HC1 scg₂₀ is 2.23 times greater than the PLA/HC0 scg₂₀ structure, while the second level of hierarchy demonstrated an increase of 2.71 times the stiffness of the regular honeycomb structure.

The result of stiffening from zero to the second-level hierarchy has also been investigated in order to determine the stress performance of FFF-printed hierarchical honeycombs. This was accomplished by curve fitting the compressive experimental results with FEA-generated data. In order to ensure the mesh-independent response, a convergence study was performed. The accuracy of the mesh sensitivity is also determined by the curve fitting of the experimental force–displacement data. Based on the convergence results performed for an elastic response of the honeycomb structures, a minimum element size of 0.86 mm was considered to be adequate to obtain acceptable accuracy in the calculated responses.

In the current FE analyses, up to 96,845 nodes and 16,917 hexahedral elements (SOLID186) were used for the generated mesh. The degrees of freedom for each node for SOLID186 is three. The curve-fitted force–displacement data obtained from the FEA are shown in Figure 7a, where it can clearly be seen that these values agree with the measured curves. Therefore, the initial values of the multilinear stress–strain model of the honeycomb structures were correct assumptions. The deformation behavior of the PLA specimens compared to the PLA sandwich specimens is shown in Figure 7b,c, respectively. The maximum deflection matches the experimental value for both cases. Similar results have been discussed in other works [40–43] where the contribution of the skins is essential for the structural integrity of the specimens.

The starch skin panels reinforced the bending strength of the PLA honeycombs, since the maximum stress observed for the PLA (without skins) was calculated to be 1.73 MPa and the corresponding response for the zeroth-, first- and second-level hierarchies of the sandwich structures was reported to be 2.20, 2.90 and 3.33 MPa, respectively. The FEA results of the deformation along with the equivalent von Mises stresses of the second level of hierarchical sandwich specimens are demonstrated in Figure 8a,b, respectively. Compared to other studies [9,10], the sandwich structures of biodegradable composites of the current work showed improved physical and mechanical properties with a greater increase in flexural strength.

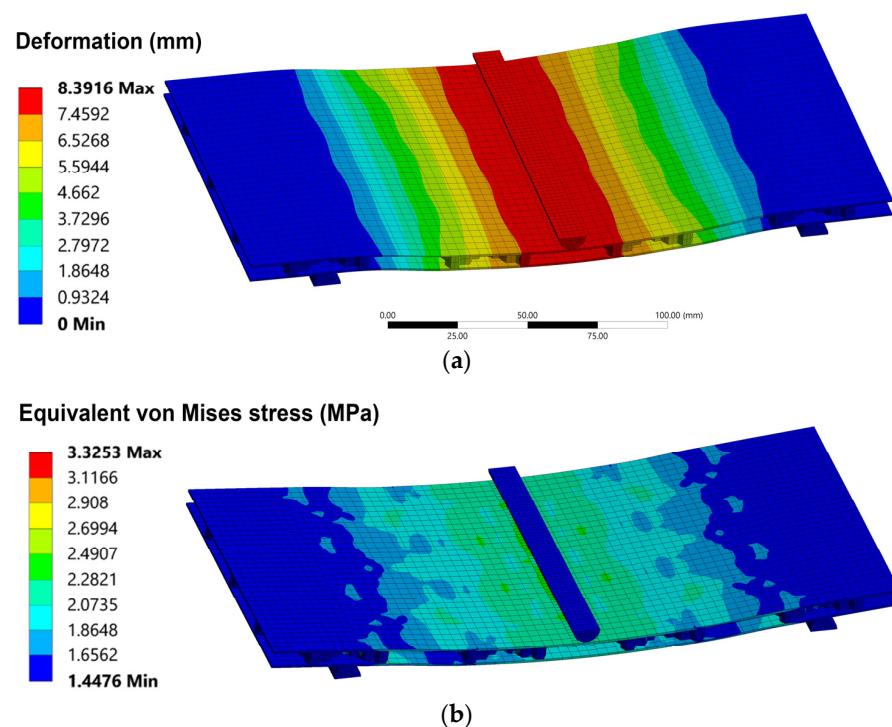


Figure 8. (a) Deformation and (b) equivalent von Mises stresses for the second level of hierarchical sandwich specimens under bending load.

4. Conclusions

In the current study, a series of biodegradable starch-based sandwich structures were manufactured. Two starch-based nanocomposite films were made as skins by a solution mixture procedure with glycerol and water as the plasticizer, containing sodium montmorillonite (NaMMT) clay, cellulose fibers and fiberglass fabric as the reinforcing fillers. The most suitable films for sandwich skins were obtained with 3 wt% NaMMT and 10 wt% cellulose, at a glycerol concentration of about 20 wt% and fiberglass fabric (with irregular structure). Three different hierarchical honeycomb cores were designed and manufactured using PLA through the FFF printing technique, HC0 for the regular honeycomb, HC1 for the first level of hierarchy and HC2 for the second level of hierarchy, to investigate the mechanical properties of starch-based sandwich structures. A sandwich with the HC0 core demonstrated better values of the neat HC0 PLA honeycomb structure (2.2 and 1.73 MPa, respectively). A HC2 core reinforced further the flexural strength of the samples, up to 3.33 MPa. It is concluded that starch-based films as skins are suitable for the fabrication of biodegradable sandwich structures, with increased strength for the 2nd order hierarchy of the honeycomb core.

Author Contributions: Conceptualization, D.T. and G.M.; methodology, M.Z., K.T. and D.T.; software, K.T.; validation, M.Z., M.T.M., K.T. and D.T.; formal analysis, M.Z. and M.T.M.; investigation, M.Z. and K.T.; resources, M.T.M.; data curation, M.Z., K.T. and D.T.; writing—original draft preparation, M.Z., K.T.; writing—review and editing, M.Z., K.T. and D.T.; visualization, M.Z. and M.T.M.; supervision, D.T. and G.M.; project administration, G.M.; funding acquisition, M.Z. All authors have read and agreed to the published version of the manuscript.

Funding: This research is co-financed by Greece and the European Union (European Social Fund-ESF) through the Operational Programme «Human Resources Development, Education and Lifelong Learning» in the context of the project “Strengthening Human Resources Research Potential via Doctorate Research” (MIS-5000432), implemented by the State Scholarships Foundation (IKY).

Conflicts of Interest: The authors declare no conflict of interest.

References

- Mouritz, A.P.; Gellert, E.; Burchill, P.; Challis, K. Review of advanced composite structures for naval ships and submarines. *Compos. Struct.* **2001**, *53*, 21–42. [[CrossRef](#)]
- Gardner, N.; Wang, E.; Shukla, A. Performance of functionally graded sandwich composite beams under shock wave loading. *Compos. Struct.* **2012**, *94*, 1755–1770. [[CrossRef](#)]
- Gupta, S.; Shukla, A. Blast performance of marine foam core sandwich composites at extreme temperatures. *Exp. Mech.* **2012**, *52*, 1521–1534. [[CrossRef](#)]
- Wijker, J. Chapter: Sandwich Construction. In *Spacecraft Structures*, 1st ed.; Springer: Berlin/Heidelberg, Germany, 2008; pp. 157–173.
- Singha, A.S.; Thakur, V.K. Mechanical properties of natural fiber reinforced polymer composites. *Bull. Mater. Sci.* **2008**, *31*, 791–799. [[CrossRef](#)]
- Singha, A.S.; Thakur, V.K. Chemical resistance, mechanical and physical properties of biofibers-based polymer composites. *Polym. Plast. Technol. Eng.* **2009**, *48*, 736–744. [[CrossRef](#)]
- Pinto, M.; Chalivendra, V.B.; Kim, Y.K.; Lewis, A.F. Effect of surface treatment and Z-axis reinforcement on the interlaminar fracture of jute/epoxy laminated composites. *Eng. Fract. Mech.* **2013**, *114*, 104–114. [[CrossRef](#)]
- Pinto, M.; Chalivendra, V.B.; Kim, Y.K.; Lewis, A.F. Evaluation of surface treatment and fabrication methods for jute fiber/epoxy laminar composites. *Polym. Compos.* **2014**, *35*, 310–317. [[CrossRef](#)]
- Bach, M.R.; Chalivendra, V.B.; Alves, C.; Depina, E. Mechanical characterization of natural biodegradable sandwich materials. *J. Sandw. Struct. Mater.* **2017**, *19*, 482–496. [[CrossRef](#)]
- Jiang, L.; Walczyk, D.; McIntyre, G.; Bucinell, R.; Tudryn, G. Manufacturing of biocomposite sandwich structures using mycelium-bound cores and preforms. *J. Manuf. Processes* **2017**, *28*, 50–59. [[CrossRef](#)]
- Mansour, G.; Zoumaki, M.; Tsongas, K.; Tzetzis, D. Starch-sandstone materials in the construction industry. *Results Eng.* **2020**, *8*, 100182. [[CrossRef](#)]
- Dweib, M.A.; Hu, B.; O'Donnell, A.; Shenton, H.W.; Woola, R.P. All natural composite sandwich beams for structural applications. *Compos. Struct.* **2004**, *63*, 147–157. [[CrossRef](#)]
- Chen, Y.; Chiparus, O.; Sun, L.; Negulescu, I.; Parikh, D.V.; Calamari, T.A. Natural fibers for automotive nonwoven composites. *J. Ind. Text.* **2005**, *35*, 47–62. [[CrossRef](#)]

14. Martin, O.; Avérous, L. Poly(lactic acid): Plasticization and properties of biodegradable multi phase systems. *Polymer* **2001**, *42*, 6209–6219. [[CrossRef](#)]
15. Pramendra, K.B.; Inderdeep, S.; Jitendra, M. Development and characterization of PLA-based green composites: A review. *J. Thermoplast. Compos. Mater.* **2014**, *27*, 52–81.
16. Ramengmawii, S.; Mohammad, J.; Mohammad, A.; Hassan, F.; Sameer, A.; Naheed, S.; Suchart, S. Flexural and Dynamic Mechanical Properties of Alkali-Treated Coir/Pineapple Leaf Fibres Reinforced Polylactic Acid Hybrid Biocomposites. *J. Bionic. Eng.* **2021**, *18*, 1430–1438.
17. Ting-Ting, L.; Heng, Z.; Shih-Yu, H.; Xin, P.; Qi, L.; Shengyu, T.; Zhiwen, M.; Jia-Horng, L. Preparation and property evaluations of PCL/PLA composite films. *J. Polym. Res.* **2021**, *28*, 156.
18. Panjehpour, M.; Ali, A.A.A.; Voo, Y.L. Structural Insulated Panels: Past, Present, and Future. *EPPM-J.* **2013**, *3*, 2–8. [[CrossRef](#)]
19. Lee, J.Y.; An, J.; Chua, C.K. Fundamentals and applications of 3D printing for novel materials. *Appl. Mater Today* **2017**, *7*, 120–133. [[CrossRef](#)]
20. Haldar, A.K.; Managuli, V.; Munshi, R.; Agarwal, R.S.; Guan, Z.W. Compressive behaviour of 3D printed sandwich structures based on corrugated core design. *Mater. Today Commun.* **2021**, *26*, 101725. [[CrossRef](#)]
21. Gohari, S.; Sharifi, S.; Burvill, C.; Mouloudi, S.; Izadifar, M.; Thissen, P. Localized failure analysis of internally pressurized laminated ellipsoidal woven GFRP composite domes: Analytical, numerical, and experimental studies. *Arch. Civ. Mech.* **2019**, *19*, 1235–1250. [[CrossRef](#)]
22. Yuguo, W.; Haoji, W.; Jinhua, W.; Bin, L.; Jingyu, X.; Sheng, F. Finite element analysis of grinding process of long fiber reinforced ceramic matrix woven composites: Modeling, experimental verification and material removal mechanism. *Ceram. Int.* **2019**, *45*, 15920–15927.
23. Gohari, S.; Sharifi, S.; Vrcelj, Z. A novel explicit solution for twisting control of smart laminated cantilever composite plates/beams using inclined piezoelectric actuators. *Compos. Struct.* **2017**, *161*, 477–504. [[CrossRef](#)]
24. Gohari, S.; Mozafari, F.; Moslemi, N.; Mouloudi, S.; Sharif, S.; Rahmanpanah, H.; Burvill, C. Analytical solution of the electro-mechanical flexural coupling between piezoelectric actuators and flexible-spring boundary structure in smart composite plates. *Arch. Civ. Mech. Eng.* **2021**, *21*, 33. [[CrossRef](#)]
25. Raphaelides, S.N.; Georgiadis, N. Effect of fatty acids on the rheological behaviour of maize starch dispersions during heating. *Carbohydr. Polym.* **2006**, *65*, 81–92. [[CrossRef](#)]
26. Müller, P.; Kapin, E.; Fekete, E. Effects of preparation methods on the structure and mechanical properties of wet conditioned starch/montmorillonite nanocomposites films. *Carbohydr. Polym.* **2014**, *113*, 569–576. [[CrossRef](#)]
27. Mansour, G.; Zoumaki, M.; Marinopoulou, A.; Raphaelides, S.N.; Tzetzis, D.; Zoumakis, N. Investigation on the Effects of Glycerol and Clay Contents on the Structure and Mechanical Properties of Maize Starch Nanocomposite Films. *Stärke* **2020**, *72*, 1900166. [[CrossRef](#)]
28. Zoumaki, M.; Tzetzis, D.; Mansour, G. Development and characterization of starch—based nanocomposite materials. *IOP Conf. Ser. Mater. Sci. Eng.* **2019**, *564*, 012037. [[CrossRef](#)]
29. Mansour, G.; Zoumaki, M.; Marinopoulou, A.; Tzetzis, D.; Prevezanos, M.; Raphaelides, S. Characterization and properties of non-granular thermoplastic starch—clay biocomposite films. *Carbohydr. Polym.* **2020**, *245*, 116629. [[CrossRef](#)]
30. Mansour, G.; Zoumaki, M.; Tsongas, K.; Tzetzis, D. Microstructural and Finite Element Analysis—Assisted Nanomechanical Characterization of Maize Starch Nanocomposite Films. *Mater. Res.* **2021**, *24*, e20200409. [[CrossRef](#)]
31. Ghanbarzadeh, B.; Almasi, H.; Entezami, A.A. Physical properties of edible modified starch/carboxymethyl cellulose films. *IFSET* **2010**, *11*, 697–702. [[CrossRef](#)]
32. Lakes, R. Materials with structural hierarchy. *Nature* **1993**, *361*, 511–515. [[CrossRef](#)]
33. Ajdari, A.; Jahromi, B.H.; Papadopoulos, J.; Nayeb-Hashemi, H.; Vaziri, A. Hierarchical honeycombs with tailorable properties. *Int. J. Solids Struct.* **2012**, *49*, 1413–1419. [[CrossRef](#)]
34. Mansour, M.T.; Tsongas, K.; Tzetzis, D. The mechanical performance of 3D printed hierarchical honeycombs using carbon fiber and carbon nanotube reinforced acrylonitrile butadiene styrene filaments. *MATEC Web Conf.* **2020**, *318*, 01049. [[CrossRef](#)]
35. Mansour, M.T.; Tsongas, K.; Tzetzis, D. 3D Printed Hierarchical Honeycombs with Carbon Fiber and Carbon Nanotube Reinforced Acrylonitrile Butadiene Styrene. *J. Compos. Sci.* **2021**, *5*, 62. [[CrossRef](#)]
36. Mansour, M.T.; Tsongas, K.; Tzetzis, D.; Antoniadis, A. The in-plane compression performance of hierarchical honeycomb additive manufactured structures. *IOP Conf. Ser. Mater. Sci. Eng.* **2019**, *564*, 012015. [[CrossRef](#)]
37. ASTM D882–12; Standard Test Method for Tensile Properties of Thin Plastic Sheeting. ASTM International: West Conshohocken, PA, USA, 2012.
38. ASTM C393/C393M-20; Standard Test Method for Core Shear Properties of Sandwich Constructions by Beam Flexure. ASTM International: West Conshohocken, PA, USA, 2020.
39. Chandrashekar, A.; Shaik, H.S.; Ranjan Mishra, S.; Srivastava, T.; Pavan Kishore, M.L. Static Structural Analysis of Hybrid Honeycomb Structures Using FEA. In *Recent Trends in Mechanical Engineering*; Narasimham, G.S.V.L., Babu, A.V., Reddy, S.S., Dhanasekaran, R., Eds.; Springer: Singapore, 2020; pp. 363–375.
40. Meifeng, H.; Wenbin, H. A study on composite honeycomb sandwich panel structure. *Compos. B Eng.* **2008**, *58*, 709–713.
41. Gutiérrez, T.J.; Ollier, R.; Alvarez, V.A. Surface properties of thermoplastic starch materials reinforced with natural fillers. In *Functional Biopolymers*; Thakur, V., Thakur, M., Eds.; Springer: Berlin/Heidelberg, Germany, 2018; pp. 131–158.

42. Hussain, M.; Khan, R.; Abbas, N. Experimental and computational studies on honeycomb sandwich structures under static and fatigue bending load. *J. King Saud Univ. Sci.* **2019**, *31*, 222–229. [[CrossRef](#)]
43. Kladovasilakis, N.; Charalampous, P.; Tsongas, K.; Kostavelis, I.; Tzetzis, D.; Tzovaras, D. Experimental and Computational Investigation of Lattice Sandwich Structures Constructed by Additive Manufacturing Technologies. *J. Manuf. Mater. Process.* **2021**, *5*, 95. [[CrossRef](#)]
44. Pandey, J.K.; Singh, R.P. Green nanocomposites from renewable resources: Effect of plasticizer on the structure and material properties of clay-filled starch. *Starke* **2005**, *57*, 8–15. [[CrossRef](#)]